
AutoBSS: An Efficient Algorithm for Block Stacking Style Search

Yikang Zhang
Huawei

zhangyikang7@huawei.com

Jian Zhang
Huawei

zhangjian157@huawei.com

Zhao Zhong
Huawei

zorro.zhongzhao@huawei.com

Abstract

Neural network architecture design mostly focuses on the new convolutional operator or special topological structure of network block, little attention is drawn to the configuration of stacking each block, called Block Stacking Style (BSS). Recent studies show that BSS may also have an unneglectable impact on networks, thus we design an efficient algorithm to search it automatically. The proposed method, AutoBSS, is a novel AutoML algorithm based on Bayesian optimization by iteratively refining and clustering Block Stacking Style Coding (BSSC), which can find optimal BSS in a few trials without biased evaluation. On ImageNet classification task, ResNet50/MobileNetV2/EfficientNet-B0 with our searched BSS achieve 79.29%/74.5%/77.79%, which outperform the original baselines by a large margin. More importantly, experimental results on model compression, object detection and instance segmentation show the strong generalizability of the proposed AutoBSS, and further verify the unneglectable impact of BSS on neural networks.

1 Introduction

Recent progress in computer vision is mostly driven by the advance of Convolutional Neural Networks (CNNs). With the evolution of network architectures from AlexNet [1], VGG [2], Inception [3] to ResNet [58], the performance has been steadily improved. Early works [1, 2, 5] designed layer-based architectures, while most of the modern architectures [3, 58, 6, 57, 8, 59] are block-based. For those block-based networks, the design procedure consists of two steps: (1) designing the block structure. (2) stacking the blocks to construct a complete network architecture. The manner for stacking blocks is named as Block Stacking Style (BSS) inspired by BCS from [10]. Compared with the block structure, BSS draws little attention from the community.

The modern block-based networks are commonly constructed by stacking blocks sequentially. The backbone can be divided into several stages, thus BSS can be simply described by the number of blocks in each stage and the number of channels for each block. The general rule to set channels for each block is to double the channels when downsampling the feature maps. This rule is adopted by a lot of famous networks, such as VGG [2], ResNet [58] and ShuffleNet [11, 8]. As for the number of blocks in each stage, there is merely a rough rule that more blocks should be allocated in the middle stages [58, 57, 8]. Such human design paradigm arouses our questions: Is this the best BSS configuration for all networks? However, recent works show that BSS may have an unneglectable impact on the performance of a network [12, 10]. [12] find a kind of pyramidal BSS style which is better than the original ResNet. Even further, [10] tries to use reinforcement learning to find optimal

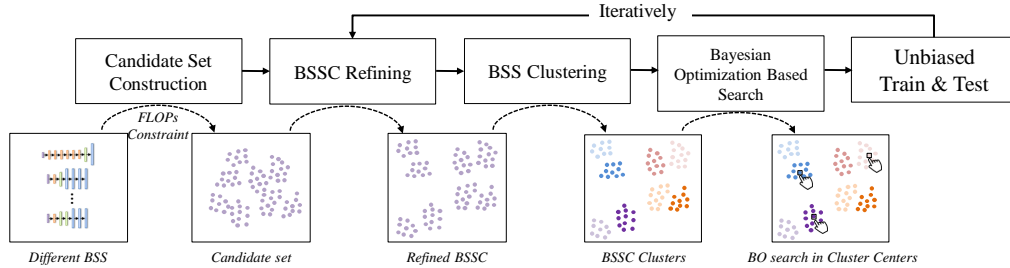


Figure 1: The overall framework of our proposed AutoBSS.

Block Connection Style (similar to BSS) for searched network block. These studies imply that the design of BSS has not been fully understood.

In this paper, we aim to break the BSS designing principles defined by human, and propose an efficient AutoML based method called **AutoBSS**. The overall framework is shown in Figure 1, where each BSS configuration is represented by Block Stacking Style Coding (BSSC). Our goal is to search an optimal BSSC with the best accuracy under some target constraints (e.g. FLOPs or latency). Current AutoML algorithms usually use a biased evaluation protocol to accelerate search [13, 14, 15, 16, 17], such as early stop or parameter sharing. However, BSS search space has its unique benefits, where BSSC has a strong physical meaning. Each BSSC affects the computation allocation of a network, thus we have an intuition that similar BSSC may have similar accuracy. Based on this intuition, we propose a Bayesian Optimization (BO) based approach. However, BO based approach does not perform well in a large discrete search space. Benefit from the strong prior, we present several methods to improve the effectiveness and sample efficiency of BO on BSS search. *BSS Clustering* aggregates BSSC into clusters, each BSSC in the same cluster have similar accuracy, thus we only need to search over cluster centers. *BSSC refining* enhances the coding representation by increasing the correlation between BSSC and corresponding accuracy. To improve BSS Clustering, we propose a candidate set construction method to select a subset from search space efficiently. Based on these improvements, AutoBSS is extremely sample efficient and only needs to train tens of BSSC, thus we use an *unbiased evaluation scheme* and avoid the strong influence caused by widely used tricks in neural architecture search (NAS) methods, such as early stopping or parameter sharing.

Experiment results on various tasks demonstrate the superiority of our proposed method. The BSS searched within tens of samplings can largely boost the performance of well-known models. On ImageNet classification task, ResNet50/MobileNetV2/EfficientNet-B0 with searched BSS achieve 79.29%/74.5%/77.79%, which outperform the original baselines by a large margin. Perhaps more surprisingly, results on model compression(+1.6%), object detection(+0.91%) and instance segmentation(+0.63%) show the strong generalizability of the proposed AutoBSS, and further verify the unneglectable impact of BSS on neural networks.

The contributions of this paper can be summarized as follows:

- We demonstrate that BSS has a strong impact on the performance of neural networks, and the BSS of current state-of-the-art networks is not the optimal solution.
- We propose a novel algorithm called AutoBSS that can find a better BSS configuration for a given network within only tens of trials. Due to the sample efficiency, AutoBSS can search with unbiased evaluation under limited computing cost, which overcomes the errors caused by the biased search scheme of current AutoML methods.
- The proposed AutoBSS improves the performance of widely used networks on classification, model compression, object detection and instance segmentation tasks, which demonstrate the strong generalizability of the proposed method.

2 Related Work

2.1 Convolutional Neural Network Design

The convolutional neural networks (CNNs) have been applied in many computer vision tasks [18, 1]. Most of modern network architectures [3, 58, 6, 57, 8] are block-based, where the design process is usually two phases: (1) designing a block structure, (2) stacking blocks to form the complete structure, in this paper we call the second phase BSS design. Many works have been devoted to effective and efficient block structure design, such as bottleneck [58], inverted bottleneck [57] and shufflenet block [8]. However, little effort has been made to BSS design, which has an unneglectable impact on network performance based on recent studies [12, 10]. There are two commonly-used rules for designing BSS: (1) doubling the channels when downsampling the feature maps, (2) allocating more blocks in the middle stages. These rough rules may not make the most potential of a carefully designed block structure. In this paper, we propose an automatic BSS search method named AutoBSS, which aims to break the human-designed BSS paradigm and find the optimal BSS configuration for a given block structure within a few trials.

2.2 Neural Architecture Search

Neural Architecture Search has drawn much attention in recent years, various algorithms have been proposed to search network architectures with reinforcement learning [19, 13, 20, 21, 22], evolutionary algorithm [23, 24], gradient-based method [25, 26] or Bayesian optimization-based method [27]. Most of these works [13, 20, 25, 24] focus on the micro block structure search, while our work focuses on the macro BSS search when the block structure is given. There are a few works related to BSS search [28, 59]. Partial Order Pruning (POP) [28] samples new BSS randomly while utilizing the evaluated BSS to prune the search space based on Partial Order Assumption. However, the search space after pruning is still too large, which makes it difficult to search BSS by random sampling. EfficientNet [59] simply grid searches three constants to scale up the width, depth, and resolution. BlockQNN [10] uses reinforcement learning to search BSS, however, it needs to evaluate thousands of BSS and uses early stop training tricks to reduce time cost. OnceForAll [29] uses weight sharing technique to progressively search the width and the depth of a supernet. The aforementioned methods are either sample inefficient or introduce some biased tricks for evaluation, such as early stop or weight sharing. Note that these tricks affect the search performance strongly [30, 31], where the correlation between the final accuracy and searched accuracy is very low. Different from those methods, our proposed AutoBSS uses an unbiased evaluation scheme and utilizes an efficient Bayesian Optimization based search method with BSS refining and clustering to find an optimal BSS within tens of trials.

3 Method

Given a building block of a neural network, BSS defines the number of blocks in each stage and channels for each block, which can be represented by a fixed-length coding, namely Block Stacking Style Coding (BSSC). BSSC has a strong physical meaning that describes the computation allocation in each stage. Thus we have a prior that similar BSSC may have similar accuracy. To benefit from this hypothesis, we propose an efficient algorithm to search BSS by Bayesian Optimization. However, BO based method does not perform well in a large discrete search space. To address this problem, we propose BSS Clustering to aggregate BSSC into clusters, and we only need to search over cluster centers efficiently. To enhance the BSSC representation, we also propose BSSC Refining to increase the correlation between coding and corresponding accuracy. Moreover, as the search space is usually huge, to perform BSS clustering efficiently, we propose Candidate Set Construction method to select a subset effectively. We will introduce these methods in the following subsections in detail.

3.1 Candidate Set Construction

The goal of AutoBSS is to search an optimal BSSC under some target constraints (e.g. FLOPs or latency). We denote the search space under the constraint as Λ . Each element of Λ is a BSSC, denoted as x , with the i -th element as x_i and the first i elements as $x_{[:i]}$, $i = 0, \dots, m$. The set of possible values for x_i is represented as $C^i = \{c_0^i, c_1^i, \dots\}$, thus $x_{[:i+1]} = x_{[:i]} \cup c_j^i, c_j^i \in C^i$. In most cases, Λ

is too large to enumerate, and clustering using the full search space is infeasible. Thus we need to select a subset of Λ as the candidate set Ω .

To make the BSS search in this subset more effectively, Ω aims to satisfy two criterions: (1) the candidates in Ω and Λ should have similar distributions. (2) the candidates in Ω should have better accuracy than the unpicked ones in the search space.

To make the distribution of candidates in Ω similar with Λ , an intuitive way is to construct Ω via random sampling in Λ . During each sampling, we can sequentially determine the value of x_0, \dots, x_m . The value of x_i is selected from C^i , where c_j^i corresponds with the possibility P_j^i . It can be proved in random sampling that,

$$P_j^i = \frac{|S(x_{[:i]} \cup c_j^i)|}{\sum_j (|S(x_{[:i]} \cup c_j^i)|)}, \text{ where } S(x_{[:r]}) = \{\hat{x} | \hat{x} \in \Lambda, \hat{x}_{[:r]} = x_{[:r]}\}. \quad (1)$$

However, we can not get the value of $|S(x_{[:r]})|$ because it needs to enumerate each element in Λ . Thus, we simply utilize the approximate value $|S^{\mathcal{D}=0}(x_{[:r]})|$ by the following equation 2 recursively, where \mathcal{D} denotes the recursion depth, c_{mid}^r denotes the median of C^r .

$$|S^{\mathcal{D}=d}(x_{[:r]})| = \begin{cases} \sum_j \{|S^{\mathcal{D}=d+1}(x_{[:r]} \cup c_j^r)|\}, & \text{if } d \leq 2 \\ |S^{\mathcal{D}=d+1}(x_{[:r]} \cup c_{mid}^r)| \times |C^r|, & \text{if } d > 2 \end{cases} \quad (2)$$

To make the candidates in Ω have better potential than the unselected ones in Λ , we post-process each candidate $x \in \Omega$ in the following manner. We first randomly select one dimension x_i , and increase it by a predefined step size if this doesn't result in larger FLOPs or latency than the threshold. This process is repeated until no dimension can be increased. Increasing any dimension x_i means increasing the number of channels or blocks, as shown in works like [57, 8, 12], it necessarily makes the resulting network perform better.

3.2 BSSC Refining

To demonstrate the correlation between BSSC and accuracy, we randomly sample 220 BSS for ResNet18 and evaluate them on ImageNet classification task. To make the distance between BSSC reasonable, we firstly standardize each dimension individually, i.e. replacing each element with Z-score. This procedure can be regarded as the first refining. Then, we show the relationship between Euclidean distance and accuracy discrepancy (the absolute difference of two accuracies) in Figure 2.

It can be observed that accuracy discrepancy tends to increase when distance gets larger, this phenomenon verifies our intuition that similar BSSC has similar accuracy. However the correlation is nonlinear. Because the Bayesian Optimization approach is based on Lipschitz-continuous assumption [53], we should refine it to a linear correlation so that the assumption can be satisfied better. Therefore, we utilize evaluated BSS to refine BSSC from the second search iteration. We simply use a linear layer to transform it in this work. We set the initial weight of this linear layer as an identity matrix, and train the model with the following loss,

$$Loss_{dy} = \left(\frac{|y^{(0)} - y^{(1)}|}{|y^{(2)} - y^{(3)}|} - \frac{\|\hat{x}^{(0)} - \hat{x}^{(1)}\|_{L_2}}{\|\hat{x}^{(2)} - \hat{x}^{(3)}\|_{L_2}} \right)^2, \quad (3)$$

where $\hat{x}^{(0)}, \dots, \hat{x}^{(3)}$ are transformed from four randomly selected evaluated BSSC and $y^{(0)}, \dots, y^{(3)}$ are the corresponding accuracies.

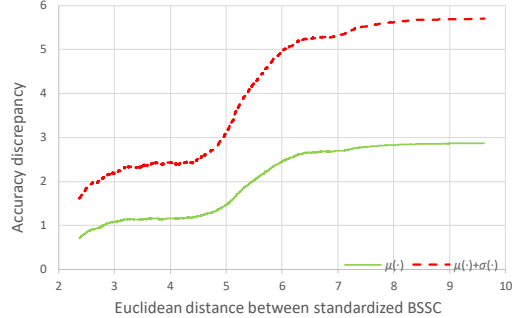


Figure 2: The relationship between BSSC distance and accuracy discrepancy. $\mu(\cdot)$ and $\sigma(\cdot)$ represent mean value and standard deviation respectively.

3.3 BSS Clustering

After refining, neighboring BSSC naturally corresponds with similar accuracies. Thus searching from the whole candidate set is not necessary. We aggregate BSSC into clusters and search from the cluster centers efficiently. Besides, it brings two extra benefits. Firstly, it helps to avoid the case that all BSSC are sampled from a local minimum. Secondly, it makes the sampled BSSC dispersed enough, thus the GP model built on which can better handle the whole candidate set.

We adopt the k-means algorithm [33] with Euclidean distance to aggregate the refined BSSC. The number of clusters will increase during each iteration, while we only select the same number of BSSC from cluster centers in each iteration. It is because the refined BSSC can measure the accuracy discrepancy more precisely and the GP model becomes more reliable with the increase of evaluated BSSC.

3.4 Bayesian Optimization Based Search

We build a model for the accuracy as $f(x)$ based on GP. Because the refined BSSC has a relatively strong correlation with accuracy, we simply use a simple kernel $\kappa(x, x') = \exp(-\frac{1}{2\sigma^2}\|x - x'\|_{L_2}^2)$. We adopt expected improvement (EI) as the acquisitions. Given $\mathcal{O} = \{(x^{(0)}, y^{(0)}), (x^{(1)}, y^{(1)}), \dots, (x^{(n)}, y^{(n)})\}$, where $x^{(i)}$ is a refined BSSC for an evaluated BSS, $y^{(i)}$ is the corresponding accuracy. Then,

$$\varphi_{EI}(x) = \mathbb{E}(\max\{0, f(x) - \tau | \mathcal{O}\}), \tau = \max_{i \leq n} y^{(i)}. \quad (4)$$

To reduce the time consumption and take advantage of parallelization, we train several different networks at a time. Therefore, we use the expected value of EI function (EEI, [54]) to select a batch of unevaluated BSSC from cluster centers. Supposing $x^{(n+1)}, x^{(n+2)}, \dots$ are BSSC for selected BSS with unknown accuracies $\hat{y}^{(n+1)}, \hat{y}^{(n+2)}, \dots$, thus

$$\varphi_{EEI}(x) = \mathbb{E}(\mathbb{E}(\max\{0, f(x) - \tau | \mathcal{O}, (x^{(n+1)}, \hat{y}^{(n+1)}), (x^{(n+2)}, \hat{y}^{(n+2)}), \dots\})), \quad (5)$$

here $\hat{y}^{(n+j)}, j = 1, 2, \dots$, is a variable of Gaussian distribution with mean and variance depend on $\{\hat{y}^{(n+k)} | 1 \leq k < j\}$. The value of equation 5 is calculated by Monte Carlo simulations [54] at each cluster center, the one with the largest value will be selected. More details are illustrated in Appendix A.1.

4 Experiments

In this section, we conduct the main experiments of BSS search on ImageNet classification task [35]. Then we conduct experiments to analyze the effectiveness of BSSC Refining and BSS Clustering. Finally, we extend the experiments to model compression, detection and instance segmentation to verify the generalization of AutoBSS. The detailed settings of experiments are demonstrated in the Appendix B.

4.1 Implementation Details

Target networks and Training hyperparameters We use ResNet18/50 [58], MobileNetV2 [57] and EfficientNet-B0/B1 [59] as target networks, and utilize AutoBSS to search a better BSS configuration for corresponding networks under the constraint of FLOPs. The detailed training settings are shown in Appendix B.1.

Definition of BSSC We introduce the definition of BSSC for EfficientNet-B0/B1 as an example, others are introduced in Appendix B.2. The main building block of EfficientNet-B0 is MBConv [57], but swish [36] and squeeze-and-excitation mechanism [37] are added. Then EfficientNet-B1 is constructed by grid searching three constants to scale up EfficientNet-B0. EfficientNet-B0/B1 consists of 9 stages, the BSSC is defined as the tuple $\{C_3, \dots, C_8, L_3, \dots, L_8, T_3, \dots, T_8\}$, C_i, L_i and T_i denote the output channels, number of blocks and expansion factor[57] for stage i , respectively.

Table 1: Single crop Top-1 accuracy (%) of different BSS configurations on ImageNet dataset

Method	FLOPs	Params	Impl. (120 ep.)	Ref.	Impl. (350 ep.)
ResNet18	1.81B	11.69M	71.21	69.00[28])	72.19
ResNet18 ^{Rand}	1.74B	24.87M	72.34	-	-
ResNet18 ^{AutoBSS}	1.81B	16.15M	73.22	-	73.91
ResNet50	4.09B	25.55M	77.09	76.00[59]	77.69
ResNet50 ^{Rand}	3.69B	23.00M	77.48	-	-
ResNet50 ^{AutoBSS}	4.03B	23.73M	78.17	-	79.29
MobileNetV2	300M	3.50M	72.13	72.00[57]	73.90
MobileNetV2 ^{Rand}	298M	4.00M	72.13	-	-
MobileNetV2 ^{AutoBSS}	296M	3.92M	72.96	-	74.50
EfficientNet-B0	385M	5.29M	-	77.10[59]	77.12
EfficientNet-B0 ^{Rand}	356M	6.67M	-	-	76.73
EfficientNet-B0 ^{AutoBSS}	381M	6.39M	-	-	77.79
EfficientNet-B1	685M	7.79M	-	79.10[59]	79.19
EfficientNet-B1 ^{Rand}	673M	10.19M	-	-	78.56
EfficientNet-B1 ^{AutoBSS}	684M	10.17M	-	-	79.48

Detail Settings of AutoBSS Searching We use FLOPs of original BSS as the threshold for Candidate Set Construction. The candidate set Ω always has 10000 elements in all experiments. The number of iterations is set as 4, during each iteration 16 BSSC will be evaluated, so that in total *only 64 networks* will be trained in the searching process. Benefit from the sample efficiency, we use an *unbiased evaluation scheme* for searching, namely each candidate is trained fully without early stopping or parameter sharing. We train 120 epochs for ResNet18/50 and MobileNetV2, 350 epochs for EfficientNet-B0/B1. We set the number of clusters as 16, 160, $\frac{N}{10}$ and N for each iteration, here N denotes the size of candidate set Ω . As indicated in [38], random search is a hard baseline to beat for NAS. Therefore we also randomly sample 64 BSSC from the same search space as a baseline for each network.

4.2 Results and Analysis

The results of ImageNet are shown in Table 1. More details are shown in Appendix B.3. Compared with the original ResNet18, ResNet50 and MobileNetV2, we improve the accuracy by **2.01%**, **1.08%** and **0.83%** respectively. It indicates BSS has an unneglectable impact on the performance, and there is a large improvement room for the manually designed BSS.

EfficientNet-B0 is developed by leveraging a reinforcement learning-based NAS approach [20, 59], BSS is involved in their search space as well. Our method achieves 0.69% improvement. The reinforcement learning-based approach needs tens of thousands of samplings while our method needs only 64 samplings, which is much more efficient. In addition, the 0.38% improvement on EfficientNet-B1 demonstrates the superiority of our method over grid search, which indicates that AutoBSS is a more elegant and efficient tool for scaling neural networks.

ResNet18/50^{Rand}, MobileNetV2^{Rand} and EfficientNet-B0/B1^{Rand} in Table 1 are networks with the randomly searched BSS, the accuracy for them is 0.88/0.69%, 0.83% and 1.06/0.92% lower compared with our proposed AutoBSS. It indicates that our method is superior to the hard baseline random search for NAS [38].

We also visualize the searching process of ResNet18 in Figure 3 (a), where each point represents a BSS. The searching process consists of 4 iterations, during each iteration, 16 evaluated BSS will be sorted based on the accuracy for better visualization. From the figure, we have two observations:

- 1) The searched BSS within the first iteration is already relatively good. It mainly comes from two points. Firstly, Candidate Set Construction excludes a large number of BSS which are expected to have a bad performance. Secondly, BSS Clustering helps to avoid the case that all BSS are sampled from a local minimum.

- 2) The best BSS is sampled during the last two iterations. It is because the growing number of evaluated BSS makes the refined BSSC and GP model more effective. As for why the best BSS is not always sampled during the last iteration, it is because we adopt EI acquisition function [53], which focuses on not only exploitation but also exploration.

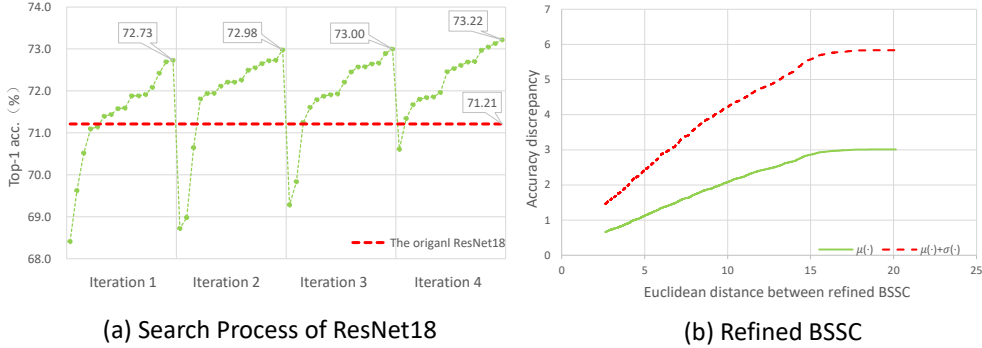


Figure 3: (a) The searching process of ResNet18. (b) Correlation between refined BSSC and accuracy

4.3 Analysis for BSSC Refining and BSS Clustering

To demonstrate the effectiveness of BSSC Refining, we use the same BSS for ResNet18 as section 3.2 to plot relations between refined BSSC distance and network accuracy in Figure 3(b). The linear model for refining is trained with 16 randomly selected BSSC and makes the mapping from refined BSSC to accuracy satisfy the Lipschitz-continuous assumption of Bayesian Optimization approach [53]. That is, there exists constant C , such that for any two refined BSSC x_1, x_2 : $|Acc(x_1) - Acc(x_2)| \leq C\|x_1 - x_2\|$. The red dashed line in Figure 2 and Figure 3(b) (mean value plus standard deviation) can be regarded as the upper bound of accuracy discrepancy $|Acc(x_1) - Acc(x_2)|$. After refined with the linear model, it becomes much more close to the form of $C\|x_1 - x_2\|$.

To prove the effectiveness of BSS Clustering, we simply carry out an experiment to search the BSS of ResNet18 without BSS Clustering. We compare the best 5 BSS in Table 2. It can be observed that the accuracy drops significantly without the BSS clustering.

Table 2: The best 5 BSS searched with/without BSS Clustering.

	Without BSS Clustering	With BSS Clustering
Top-1 acc. (%)	72.56 (0.42 ↓)	72.98
	72.59 (0.41 ↓)	73.00
	72.60 (0.45 ↓)	73.05
	72.63 (0.50 ↓)	73.13
	72.70 (0.52 ↓)	73.22
Mean(%)	72.62 (0.46 ↓)	73.08

4.4 Generalization to Model Compression

Model compression aims to obtain a smaller network based on a given architecture. By adopting a smaller FLOPs threshold, model compression can be achieved with our proposed AutoBSS as well. We conduct an experiment on MobileNetV2, settings are identical with section 4.1 except for FLOPs threshold and training epochs. We compare our method with Meta Pruning [39], ThiNet [40] and Greedy Selection [41]. The results are shown in Table 3, AutoBSS improves the accuracy by a large margin. It indicates that pruning based methods is less effective than scaling a network using AutoBSS.

Table 3: Compared with other methods on MobileNetV2.

Method	FLOPs	Params	Top-1 acc. (%)
Uniformly Rescale	130M	2.2M	68.05
Meta Pruning [39]	140M	-	68.20 [39]
ThiNet [40]	175M	-	68.60 [41]
Greedy Selection [41]	137M	2.0M	68.80 [41]
AutoBSS(ours)	130M	2.7M	69.65

4.5 Generalization to Detection and Instance Segmentation

To investigate whether our method generalizes beyond the classification task, we also conduct experiments to search the BSS for the backbone of RetinaNet-R50 [42] and Mask R-CNN-R50 [43] on detection and instance segmentation task. We report results on COCO dataset [60]. As pointed out in [45] that ImageNet pre-training speeds up convergence but does not improve final target task accuracy, we train the detection and segmentation model **from scratch**, using SyncBN [61] with a 3x scheduler. The detailed settings are shown in Appendix B.4. The results are shown in Table 4. We can see that both AP^{bbox} and AP^{mask} are improved for Mask R-CNN with our searched BSS. AP^{bbox} is improved by 0.91% and AP^{mask} is improved by 0.63%. Moreover, AP^{bbox} for RetinaNet is improved by 0.66% as well. This indicates that our method can generalize well beyond classification task.

Table 4: Comparison between the original BSS and the one searched by our method.

Backbone	FLOPs	Params	AP^{bbox} (%)	AP^{mask} (%)
Mask R-CNN-R50	117B	44M	39.24	35.74
Mask R-CNN-R50 ^{AutoBSS}	116B	49M	40.15	36.37
RetinaNet-R50	146B	38M	37.02	-
RetinaNet-R50 ^{AutoBSS}	146B	41M	37.68	-

4.6 Generalization for Searched BSSC to Similar Task

To investigate whether the searched BSSC can generalize to a similar task, we experiment on generalizing the BSSC searched for Mask R-CNN-R50 on instance segmentation task to semantic segmentation task. We report results on PSACAL VOC 2012 dataset [47] for PSPNet [48] and PSANet [49]. Our models are pre-trained on ImageNet and finetuned on train_aug (10582 images) set. The experiment settings are identical with [50] and results are shown in Table 5. We can see that both PSPNet50 and PSANet50 are improved equipped with the searched BSSC. It shows that the searched BSSC can generalize to a similar task.

Table 5: The single scale testing results on PSACAL VOC 2012.

Method	mIoU (%)	mAcc (%)	aAcc (%)
PSPNet50	77.05	85.13	94.89
PSPNet50 ^{AutoBSS}	78.22	86.50	95.18
PSANet50	77.25	85.69	94.91
PSANet50 ^{AutoBSS}	78.04	86.79	95.03

4.7 Qualitative Analysis for the Searched BSS

We further analyze the searched BSS configuration and give more insights. We compare the searched BSS with the original one in Figure 4. We can observe that the computation allocated uniformly for different stages in the original BSS configuration. This rule is widely adopted by many modern neural networks [58, 11, 8]. However, the BSS searched by AutoBSS presents a different pattern. We can observe some major differences from the original one:

- 1) The computation cost is not uniformly distributed, AutoBSS assign more FLOPs in latter stages. We think maybe the low-level feature extraction in shallow layers may not need too much computation, while the latter semantic feature may be more important.
- 2) AutoBSS increases the depth of early stages by stacking a large number of narrow layers, we think it may indicate that a large receptive field is necessary for early stages.
- 3) AutoBSS uses only one extremely wide block in the last stage, which may indicate that semantic features need more channels to extract delicately.

By the comparison of original BSS and the automatically searched one, we can observe that the human-designed principle for stacking blocks is not optimal. The uniform allocation rule can not make the most potential of computation.

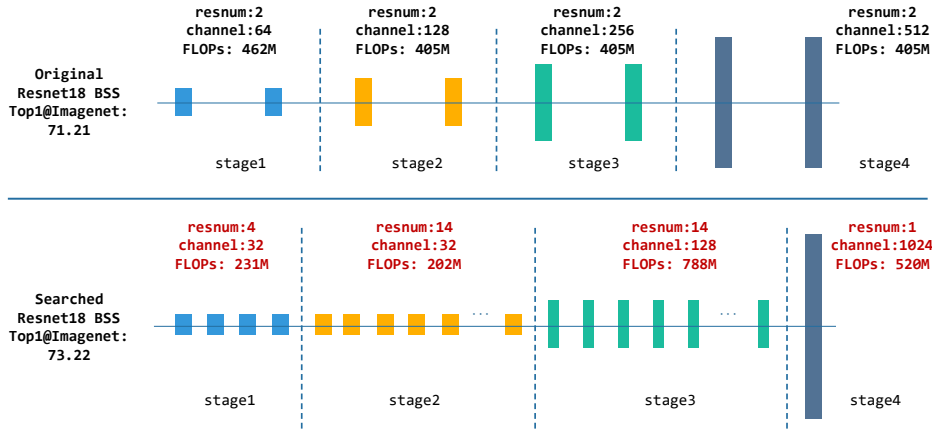


Figure 4: The difference between the original BSS and the searched one on ResNet18.

5 Conclusion

In this paper, we focus on the search of Block Stacking Style (BSS) of a network, which has drawn little attention from researchers. We propose a Bayesian optimization based search method named AutoBSS, which can efficiently find a better BSS configuration for a given network within tens of trials. We demonstrate the effectiveness and generalizability of AutoBSS with various network backbones on different tasks, including classification, model compression, detection and segmentation. The results show that AutoBSS improves the performance of well-known networks by a large margin. We analyze the searched BSS and give insights that BSS affects the computation allocation of a neural network, and different networks have different optimal BSS. This work highlights the impact of BSS on network design and NAS. In the future, we plan to further analyze the underlying impact of BSS on network performance. Another important future research topic is searching the BSS and block topology of a neural network jointly, which will further promote the performance of neural networks.

Broader Impact

The main goal of this work is to investigate the impact of Block Stacking Style (BSS) and design an efficient algorithm to search it automatically. As shown in our experiments, the BSS configuration of current popular networks is not the optimal solution. Our methods can give a better understanding of the neural network design and exploit their capabilities. For the community, one potential positive impact of our work would be that we should not only focus on new convolutional operator or topological structure but also BSS of the Network. In addition, our work indicates that AutoML algorithm with unbiased evaluation has a strong potential for future research. For the negative aspects, our experiments on model compression may suggest that pruning based methods have less potential than tuning the BSS of a network.

A Additional Details for AutoBSS

A.1 Bayesian Optimization Based Search

In this procedure, we build a model for the accuracy of unevaluated BSSC based on evaluated one. Gaussian Process (GP, [51]) is a good method to achieve this in Bayesian optimization literature [52]. A GP is a random process defined on some domain \mathcal{X} , and is characterized by a mean function $\mu : \mathcal{X} \rightarrow R$ and a covariance kernel $\kappa : \mathcal{X}^2 \rightarrow R$. In our method, $\mathcal{X} \in R^m$, where m is the dimension of BSSC.

Given $\mathcal{O} = \{(x^{(0)}, y^{(0)}), (x^{(1)}, y^{(1)}), \dots, (x^{(n-1)}, y^{(n-1)})\}$, where $x^{(i)}$ is a refined BSSC for an evaluated BSS, $y^{(i)}$ is the corresponding accuracy. We firstly standardize $y^{(i)}$ to $\hat{y}^{(i)}$ whose prior distribution has mean 0 and variance $1 + \eta^2$ so that $\hat{y}^{(i)}$ can be modeled as $\hat{y}^{(i)} = f(x^{(i)}) + \epsilon_i$, here f is a GP with $\mu(x) = 0$ and $\kappa(x, x') = \exp(-\frac{1}{2\sigma^2} \|x - x'\|_{L_2}^2)$, $\epsilon_i \sim N(0, \eta^2)$ is the white noise term, σ and η are hyperparameters. Considering that the variance of ϵ_i should be much smaller than the variance of $\hat{y}^{(i)}$, we simply set $\eta = 0.1$ in our method. σ determines the sharpness of the fall-off for kernel function $\kappa(x, x')$ and is determined dynamically based on the set \mathcal{O} , the details are illustrated below.

Firstly, we calculate the mean accuracy discrepancy for the BSSC evaluated in the first iteration. Because they are dispersed clustering centers, the mean discrepancy is relatively large. Then, we utilize this value to filter \mathcal{O} and get the pairs of BSSC with a larger accuracy discrepancy than it. Afterward, we calculate the BSSC distance for the pairs and sort them to get $\{Dis_0, Dis_1, \dots, Dis_{l-1}\}$, where $Dis_0 < Dis_1 < \dots < Dis_{l-1}$. Finally, σ is set as $\frac{Dis_{\frac{l}{20}}}{2}$.

It can be derived that the posterior process $f|\mathcal{O}$ is also a GP, we denote its mean function and kernel function as μ_n and κ_n respectively. Denote $Y \in R^n$ with $Y_i = \hat{y}^{(i)}$, $k, k' \in R^n$ with $k_i = \kappa(x, x^{(i)})$, $k'_i = \kappa(x', x^{(i)})$, and $K \in R^{n \times n}$ with $K_{i,j} = \kappa(x^{(i)}, x^{(j)})$. Then, μ_n, κ_n can be computed via,

$$\mu_n(x) = k^T (K + \eta^2 I)^{-1} Y, \quad \kappa_n(x, x') = \kappa(x, x') - k^T (K + \eta^2 I)^{-1} k'. \quad (6)$$

The value of posterior process $f|\mathcal{O}$ on each unevaluated BSS is a Gaussian distribution, whose mean and variance can be computed via equation 6. This distribution can measure the potential for each unevaluated BSSC. To determine the BSSC for evaluation, an acquisition function $\varphi : \mathcal{X} \rightarrow R$ is introduced, the BSSC with the maximum φ value will be selected. There are kinds of acquisitions [53], we use expected improvement (EI) in this work,

$$\varphi_{EI}(x) = \mathbb{E}(\max\{0, f(x) - \tau|\mathcal{O}\}), \tau = \max_{i < n} (\hat{y}^{(i)}). \quad (7)$$

EI measures the expected improvement over the current maximum value according to the posterior GP.

To reduce the time consumption and take advantage of parallelization, we train several different networks at a time. When selecting the first BSSC, equation 7 can be used directly. However, when selecting the following ones, there arises the problem that the accuracies for some BSSC are still unknown. Therefore, we use the expected value of EI function (EEI, [54]) instead. Supposing $x^{(n)}, x^{(n+1)}, \dots$ are BSSC for selected BSS with unknown accuracies $\tilde{y}^{(n)}, \tilde{y}^{(n+1)}, \dots$, thus

$$\varphi_{EEI}(x) = \mathbb{E}(\mathbb{E}(\max\{0, f(x) - \tau|\mathcal{O}, (x^{(n)}, \tilde{y}^{(n)}), (x^{(n+1)}, \tilde{y}^{(n+1)}), \dots\})), \quad (8)$$

here $\tilde{y}^{(n+j)}$ is a variable of Gaussian distribution with mean and variance depend on $\tilde{y}^{(n)}, \dots, \tilde{y}^{(n+j-1)}$. The value of equation 8 is calculated via Monte Carlo simulations [54] in our method.

B Additional Details for Experiments

B.1 Settings for the training networks on ImageNet

To study the performance of our method, a large number of networks are trained, including networks with original BSS and the ones with sampled BSS. The specifics are shown in Table 6

Table 6: Settings for the training networks on ImageNet.

Shared	Optimizer: SGD	Batch size: 1024		
	Lr strategy: Consin[55]	Label smooth: 0.1		
	Weight decay	Initial Lr	Num of epochs	Augmentation
ResNet18	0.00004	0.4	120	-
ResNet50	0.0001	0.7	120	-
MobileNetV2	0.00002	0.7	120	-
EfficientNet-B0	0.00002	0.7	350	Fixed AutoAug[56]
EfficientNet-B1	0.00002	0.7	350	Fixed AutoAug[56]

B.2 Additional Details for the Definition of BSSC

B.2.1 Definition of BSSC for ResNet18/50 and MobileNetV2

The definition of BSSC for EfficientNet-B0/B1 has been introduced in paper. Here we demonstrate the ones for ResNet18/50 and MobileNetV2.

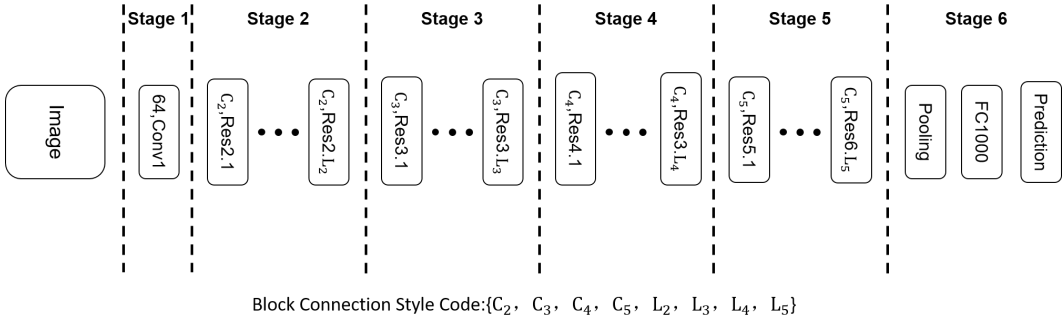


Figure 5: The backbone of ResNets. L_2, L_3, L_4, L_5 are number of blocks for each stage, C_2, C_3, C_4, C_5 are the corresponding output channels.

ResNet18/50 consists of 6 stages as illustrated in Figure 5. Stages 1~5 down-sample the spatial resolution of input tensor, stage 6 produces the final prediction by a global average pooling and a fully connected layer. The BSSC for ResNet18 is defined as the tuple $\{C_2, \dots, C_5, L_2, \dots, L_5\}$, where C_i denotes the output channels, L_i denotes the number of residual blocks. As for the BSSC of ResNet50, we utilize B_i to describe the bottleneck channels for stage i , thus it becomes $\{C_2, \dots, C_5, L_2, \dots, L_5, B_2, \dots, B_5\}$.

MobileNetV2 consists of 9 stages, its main building block is mobile inverted bottleneck MBConv [57]. The specifics is shown in Table 7. In our experiment, the BSSC for MobileNetV2 is defined as the tuple $\{C_3, \dots, C_8, L_3, \dots, L_8, T_3, \dots, T_8\}$. C_i, L_i and T_i denote the output channels, number of blocks and expansion factor[57] for stage i respectively.

B.2.2 Constraints on the BSSC

For the BSSC of ResNet18, we constrain $\{C_2, \dots, C_5\}$ to be the power of 2, with the minimum as $\{2^5, 2^5, 2^6, 2^7\}$ and maximum as $\{2^8, 2^{10}, 2^{11}, 2^{11}\}$. Moreover, the range of $L_i, i = 2, \dots, 5$ is constrained to be $[1, 16]$. For the BSSC of ResNet50, we constrain $\{C_2, \dots, C_5\}$ to be

Table 7: MobileNetV2 network. Each row describes a stage i with L_i layers, with input resolution $H_i \times W_i$, expansion factor[57] T_i and output channels C_i .

Stage i	Operator F_i	Resolution $H_i \times W_i$	Expansion factor T_i	Channels C_i	Layers L_i
1	Conv3x3	224×224	-	32	1
2	MBCConv,k3x3	112×112	1	16	1
3	MBCConv,k3x3	112×112	6	24	2
4	MBCConv,k3x3	56×56	6	32	3
5	MBCConv,k3x3	28×28	6	64	4
6	MBCConv,k3x3	14×14	6	96	3
7	MBCConv,k3x3	14×14	6	160	3
8	MBCConv,k3x3	7×7	6	320	1
9	Conv1x1&Pooling&FC	7×7	-	1280	1

the multiple of $\{64, 128, 256, 512\}$, with the minimum as $\{64, 128, 256, 512\}$ and maximum as $\{320, 768, 1536, 3072\}$. $L_i, i = 2, \dots, 5$ are constrained to be no larger than 11. The value of B_i is chosen from $\{\frac{C_i}{8}, \frac{C_i}{4}, \frac{3C_i}{8}, \frac{C_i}{2}\}$ for stage i .

For the BSSC of MobileNetV2, we constrain $\{C_3, \dots, C_8\}$ to be the multiple of $\{4, 8, 16, 24, 40, 80\}$, with the minimum as $\{12, 16, 32, 48, 80, 160\}$ and maximum as $\{32, 64, 128, 192, 320, 640\}$. $\{L_3, \dots, L_8\}$ are constrained to be no larger than $\{5, 6, 7, 6, 6, 4\}$. The value of expansion factor T_i is chosen from $\{3, 6\}$.

For the BSSC of EfficientNet-B0/B1, we constrain $\{C_3, \dots, C_8\}$ to be the multiple of $\{4, 8, 16, 28, 48, 80\}$, with the minimum as $\{16, 24, 48, 56, 144, 160\}$ and maximum as $\{32, 64, 160, 280, 480, 640\}$. $\{L_3, \dots, L_8\}$ are constrained to be no larger than $\{6, 6, 7, 7, 8, 5\}$. The value of expansion factor T_i is chosen from $\{3, 6\}$.

B.3 Additional Details for the Searched BSSC

B.3.1 The Searched BSSC on ImageNet

Table 8: Comparison between the original BSSC and the one searched by random search or our method.

Method	BSS Code	FLOPs	Params
ResNet18[58]	$\{64, 128, 256, 512, 2, 2, 2, 2\}$	1.81B	11.69M
ResNet18 ^{Rand}	$\{32, 64, 128, 512, 1, 2, 8, 5\}$	1.74B	24.87M
ResNet18 ^{AutoBSS}	$\{32, 32, 128, 1024, 4, 14, 14, 1\}$	1.81B	16.15M
ResNet50[58]	$\{256, 512, 1024, 2048, 3, 4, 6, 3, 64, 128, 256, 512\}$	4.09B	25.55M
ResNet50 ^{Rand}	$\{128, 640, 1024, 3072, 8, 7, 4, 3, 48, 80, 256, 384\}$	3.69B	23.00M
ResNet50 ^{AutoBSS}	$\{128, 256, 768, 2048, 9, 6, 9, 3, 48, 128, 192, 512\}$	4.03B	23.73M
MobileNetV2[59]	$\{24, 32, 64, 96, 160, 320, 2, 3, 4, 3, 3, 1, 6, 6, 6, 6, 6\}$	300M	3.50M
MobileNetV2 ^{Rand}	$\{20, 48, 80, 144, 200, 480, 2, 4, 3, 2, 5, 1, 3, 3, 3, 6, 3, 3\}$	298M	4.00M
MobileNetV2 ^{AutoBSS}	$\{24, 40, 64, 96, 120, 240, 4, 3, 2, 3, 6, 2, 3, 6, 6, 3, 6, 6\}$	296M	3.92M
EfficientNet-B0[59]	$\{24, 40, 80, 112, 192, 320, 2, 2, 3, 3, 4, 1, 6, 6, 6, 6, 6, 6\}$	385M	5.29M
EfficientNet-B0 ^{Rand}	$\{24, 40, 96, 112, 192, 640, 1, 2, 1, 2, 6, 1, 6, 6, 6, 3, 6, 6\}$	356M	6.67M
EfficientNet-B0 ^{AutoBSS}	$\{28, 48, 80, 140, 144, 240, 3, 1, 4, 2, 6, 3, 3, 3, 6, 3, 6, 6\}$	381M	6.39M
EfficientNet-B1[59]	$\{24, 40, 80, 112, 192, 320, 3, 3, 4, 4, 5, 2, 6, 6, 6, 6, 6, 6\}$	685M	7.79M
EfficientNet-B1 ^{Rand}	$\{16, 24, 128, 140, 240, 400, 4, 6, 2, 4, 5, 2, 3, 3, 3, 6, 6\}$	673M	10.19M
EfficientNet-B1 ^{AutoBSS}	$\{24, 64, 96, 112, 192, 240, 3, 1, 3, 4, 7, 5, 6, 3, 3, 3, 6, 6\}$	684M	10.17M

B.3.2 The Searched BSSC on Model Compression

Table 9: Comparison between the BSSC obtained by uniformly rescaling or AutoBSS for MobileNetV2.

Method	BSS Code	FLOPs	Params
Uniformly Rescale	{16,20,40,56,96,192,2,3,4,3,3,1,6,6,6,6,6}	130M	2.2M
AutoBSS(ours)	{16,20,40,56,96,288,1,4,6,1,6,1,3,6,6,3,6,6}	130M	2.7M

B.3.3 The Searched BSSC on Detection and Instance Segmentation

Table 10: Comparison between the original BSS and the one searched by AutoBSS.

Backbone	BSS Code	FLOPs	Params
Mask R-CNN-R50	{256,512,1024,2048,3,4,6,3,64,128,256,512}	117B	44M
Mask R-CNN-R50 ^{AutoBSS}	{192,512,512,1024,9,3,6,10,24,192,256,384}	116B	49M
RetinaNet-R50	{256,512,1024,2048,3,4,6,3,64,128,256,512}	146B	38M
RetinaNet-R50 ^{AutoBSS}	{192,384,768,1536,3,7,9,8,72,192,192,384}	146B	41M

B.4 Additional Details for Settings on Detection and Instance Segmentation

We train the models on COCO [60] train2017 split, and evaluate on the 5k COCO val2017 split. We evaluate bounding box (bbox) Average Precision (AP) for object detection and mask AP for instance segmentation.

Experiment settings Most settings are identical with the ones on ImageNet classification task, we only introduce the task specific settings here. We adopt the end-to-end fashion [61] of training Region Proposal Networks (RPN) jointly with Mask R-CNN. All models are trained from scratch with 8 GPUs, with a mini-batch size of 2 images per GPU. We train a total of 270K iterations. SyncBN [62] is used to replace all ‘frozen BN’ layers. The initial learning rate is 0.02 with 2500 iterations to warm-up [63], and it will be reduced by 10× in the 210K and 250K iterations. The weight decay is 0.0001 and momentum is 0.9. Moreover, no data augmentation is utilized for testing, and only horizontal flipping augmentation is utilized for training. The image scale is 800 pixels for the shorter side for both testing and training. The BSSC is defined as the one for ResNet50 on ImageNet classification task and we also constrain the FLOPs for the searched BSS no larger than the original one. FLOPs is calculated with an input size 800 × 800. Only backbone, FPN and RPN are taken into account for the FLOPs of Mask R-CNN-R50. In the searching procedure, we only target to search BSS for higher AP.

References

- [1] Alex Krizhevsky, Ilya Sutskever, and Geoffrey E Hinton. Imagenet classification with deep convolutional neural networks. In *Advances in neural information processing systems*, pages 1097–1105, 2012.
- [2] K. Simonyan and A. Zisserman. Very deep convolutional networks for large-scale image recognition. In *International Conference on Learning Representations*, pages 1–14, 2015.
- [3] Christian Szegedy, Wei Liu, Yangqing Jia, Pierre Sermanet, Scott Reed, Dragomir Anguelov, Dumitru Erhan, Vincent Vanhoucke, and Andrew Rabinovich. Going deeper with convolutions. In *The IEEE conference on computer vision and pattern recognition*, pages 1–9, 2015.
- [4] Kaiming He, Xiangyu Zhang, Shaoqing Ren, and Jian Sun. Deep residual learning for image recognition. In *The IEEE conference on computer vision and pattern recognition*, pages 770–778, 2016.
- [5] Yann LeCun, Léon Bottou, Yoshua Bengio, and Patrick Haffner. Gradient-based learning applied to document recognition. *Proceedings of the IEEE*, 86(11):2278–2324, 1998.
- [6] Andrew G Howard, Menglong Zhu, Bo Chen, Dmitry Kalenichenko, Weijun Wang, Tobias Weyand, Marco Andreetto, and Hartwig Adam. Mobilenets: Efficient convolutional neural networks for mobile vision applications. *arXiv preprint arXiv:1704.04861*, 2017.
- [7] Mark Sandler, Andrew Howard, Menglong Zhu, Andrey Zhmoginov, and Liang-Chieh Chen. Mobilenetv2: Inverted residuals and linear bottlenecks. In *The IEEE Conference on Computer Vision and Pattern Recognition*, pages 4510–4520, 2018.
- [8] Ningning Ma, Xiangyu Zhang, Hai-Tao Zheng, and Jian Sun. Shufflenet v2: Practical guidelines for efficient cnn architecture design. In *The European Conference on Computer Vision (ECCV)*, pages 116–131, 2018.
- [9] Mingxing Tan and Quoc V. Le. Efficientnet: Rethinking model scaling for convolutional neural networks. In *International Conference on Learning Representations*, pages 6105–6114, 2019.
- [10] Z. Zhong, Z. Yang, B. Deng, J. Yan, W. Wu, J. Shao, and C. Liu. Blockqnn: Efficient block-wise neural network architecture generation. *IEEE Transactions on Pattern Analysis and Machine Intelligence*, pages 1–1, 2020.
- [11] Xiangyu Zhang, Xinyu Zhou, Mengxiao Lin, and Jian Sun. Shufflenet: An extremely efficient convolutional neural network for mobile devices. In *The IEEE Conference on Computer Vision and Pattern Recognition*, pages 6848–6856, 2018.
- [12] Dongyoon Han, Jiwhan Kim, and Junmo Kim. Deep pyramidal residual networks. In *The IEEE Conference on Computer Vision and Pattern Recognition*, pages 5927–5935, 2017.
- [13] Barret Zoph, Vijay Vasudevan, Jonathon Shlens, and Quoc V Le. Learning transferable architectures for scalable image recognition. In *The IEEE conference on computer vision and pattern recognition*, pages 8697–8710, 2018.
- [14] Yukang Chen, Gaofeng Meng, Qian Zhang, Shiming Xiang, Chang Huang, Lisen Mu, and Xinggang Wang. Renas: Reinforced evolutionary neural architecture search. In *Proceedings of the IEEE/CVF Conference on Computer Vision and Pattern Recognition (CVPR)*, June 2019.
- [15] Jiemin Fang, Yuzhu Sun, Qian Zhang, Yuan Li, Wenyu Liu, and Xinggang Wang. Densely connected search space for more flexible neural architecture search. In *Proceedings of the IEEE/CVF Conference on Computer Vision and Pattern Recognition (CVPR)*, June 2020.
- [16] Wuyang Chen, Xinyu Gong, Xianming Liu, Qian Zhang, Yuan Li, and Zhangyang Wang. Fasterseg: Searching for faster real-time semantic segmentation. In *International Conference on Learning Representations*, 2020.
- [17] Muyuan Fang, Qiang Wang, and Zhao Zhong. Betanas: Balanced training and selective drop for neural architecture search, 2019.
- [18] Christian Szegedy, Alexander Toshev, and Dumitru Erhan. Deep neural networks for object detection. In *Advances in neural information processing systems*, pages 2553–2561, 2013.
- [19] Barret Zoph and Quoc V Le. Neural architecture search with reinforcement learning. In *International Conference on Learning Representations*, 2017.

- [20] Mingxing Tan, Bo Chen, Ruoming Pang, Vijay Vasudevan, Mark Sandler, Andrew Howard, and Quoc V. Le. Mnasnet: Platform-aware neural architecture search for mobile. In *The IEEE Conference on Computer Vision and Pattern Recognition*, pages 2820–2828, 2019.
- [21] Zhao Zhong, Junjie Yan, Wei Wu, Jing Shao, and Cheng-Lin Liu. Practical block-wise neural network architecture generation. In *The IEEE Conference on Computer Vision and Pattern Recognition (CVPR)*, 2018.
- [22] Minghao Guo, Zhao Zhong, Wei Wu, Dahua Lin, and Junjie Yan. Irlas: Inverse reinforcement learning for architecture search. In *Proceedings of the IEEE/CVF Conference on Computer Vision and Pattern Recognition (CVPR)*, June 2019.
- [23] Esteban Real, Sherry Moore, Andrew Selle, Saurabh Saxena, Yutaka Leon Suematsu, Jie Tan, Quoc V Le, and Alexey Kurakin. Large-scale evolution of image classifiers. In *International Conference on Machine Learning-Volume 70*, pages 2902–2911. JMLR. org, 2017.
- [24] Esteban Real, Alok Aggarwal, Yanping Huang, and Quoc V Le. Regularized evolution for image classifier architecture search. In *Proceedings of the aaai conference on artificial intelligence*, volume 33, pages 4780–4789, 2019.
- [25] Hanxiao Liu, Karen Simonyan, and Yiming Yang. Darts: Differentiable architecture search. In *International Conference on Learning Representations*, 2019.
- [26] Han Cai, Ligeng Zhu, and Song Han. Proxylessnas: Direct neural architecture search on target task and hardware. In *International Conference on Learning Representations*, 2019.
- [27] Kirthevasan Kandasamy, Willie Neiswanger, Jeff Schneider, Barnabas Poczos, and Eric P Xing. Neural architecture search with bayesian optimisation and optimal transport. In S. Bengio, H. Wallach, H. Larochelle, K. Grauman, N. Cesa-Bianchi, and R. Garnett, editors, *Advances in Neural Information Processing Systems 31*, pages 2016–2025. Curran Associates, Inc., 2018.
- [28] Xin Li, Yiming Zhou, Zheng Pan, and Jiashi Feng. Partial order pruning: for best speed/accuracy trade-off in neural architecture search. *Proceedings of the IEEE conference on computer vision and pattern recognition*, 2019.
- [29] Han Cai, Chuang Gan, and Song Han. Once for all: Train one network and specialize it for efficient deployment. *arXiv preprint arXiv:1908.09791*, 2019.
- [30] Antoine Yang, Pedro M Esperança, and Fabio M Carlucci. Nas evaluation is frustratingly hard. *arXiv preprint arXiv:1912.12522*, 2019.
- [31] Christian Sciuto, Kaicheng Yu, Martin Jaggi, Claudiu Musat, and Mathieu Salzmann. Evaluating the search phase of neural architecture search. *arXiv preprint arXiv:1902.08142*, 2019.
- [32] Eric Brochu, Vlad M. Cora, and Nando de Freitas. A tutorial on bayesian optimization of expensive cost functions, with application to active user modeling and hierarchical reinforcement learning. *CoRR*, abs/1012.2599, 2010.
- [33] James MacQueen et al. Some methods for classification and analysis of multivariate observations. In *Proceedings of the fifth Berkeley symposium on mathematical statistics and probability*, volume 1, pages 281–297. Oakland, CA, USA, 1967.
- [34] David Ginsbourger, Janis Janusevskis, and Rodolphe Le Riche. Dealing with asynchronicity in parallel Gaussian Process based global optimization. Research report, Mines Saint-Etienne, 2011.
- [35] Jia Deng, Wei Dong, Richard Socher, Li-Jia Li, Kai Li, and Li Fei-Fei. Imagenet: A large-scale hierarchical image database. In *2009 IEEE conference on computer vision and pattern recognition*, pages 248–255. Ieee, 2009.
- [36] Stefan Elfving, Eiji Uchibe, and Kenji Doya. Sigmoid-weighted linear units for neural network function approximation in reinforcement learning. *Neural Networks*, 107:3–11, 2018.
- [37] Jie Hu, Li Shen, and Gang Sun. Squeeze-and-excitation networks. In *Proceedings of the IEEE conference on computer vision and pattern recognition*, pages 7132–7141, 2018.
- [38] Liam Li and Ameet Talwalkar. Random search and reproducibility for neural architecture search. *CoRR*, abs/1902.07638, 2019.
- [39] Zechun Liu, Haoyuan Mu, Xiangyu Zhang, Zichao Guo, Xin Yang, Tim Kwang-Ting Cheng, and Jian Sun. Metapruning: Meta learning for automatic neural network channel pruning. *arXiv preprint arXiv:1903.10258*, 2019.

- [40] Jian-Hao Luo, Jianxin Wu, and Weiyao Lin. Thinet: A filter level pruning method for deep neural network compression. In *Proceedings of the IEEE international conference on computer vision*, pages 5058–5066, 2017.
- [41] Mao Ye, Chengyue Gong, Lizhen Nie, Denny Zhou, Adam Klivans, and Qiang Liu. Good subnetworks provably exist: Pruning via greedy forward selection. *arXiv preprint arXiv:2003.01794*, 2020.
- [42] Tsung-Yi Lin, Priya Goyal, Ross Girshick, Kaiming He, and Piotr Dollár. Focal loss for dense object detection. In *Proceedings of the IEEE international conference on computer vision*, pages 2980–2988, 2017.
- [43] Kaiming He, Georgia Gkioxari, Piotr Dollár, and Ross Girshick. Mask r-cnn. In *Proceedings of the IEEE international conference on computer vision*, pages 2961–2969, 2017.
- [44] Tsung-Yi Lin, Michael Maire, Serge Belongie, James Hays, Pietro Perona, Deva Ramanan, Piotr Dollár, and C Lawrence Zitnick. Microsoft coco: Common objects in context. In *European conference on computer vision*, pages 740–755. Springer, 2014.
- [45] Kaiming He, Ross Girshick, and Piotr Dollar. Rethinking imagenet pre-training. In *Proceedings of the IEEE/CVF International Conference on Computer Vision (ICCV)*, October 2019.
- [46] Shaoqing Ren, Kaiming He, Ross Girshick, and Jian Sun. Faster r-cnn: Towards real-time object detection with region proposal networks. In *Advances in neural information processing systems*, pages 91–99, 2015.
- [47] Mark Everingham, Luc Van Gool, Christopher KI Williams, John Winn, and Andrew Zisserman. The pascal visual object classes (voc) challenge. *International journal of computer vision*, 88(2):303–338, 2010.
- [48] Hengshuang Zhao, Jianping Shi, Xiaojuan Qi, Xiaogang Wang, and Jiaya Jia. Pyramid scene parsing network. In *Proceedings of the IEEE conference on computer vision and pattern recognition*, pages 2881–2890, 2017.
- [49] Hengshuang Zhao, Yi Zhang, Shu Liu, Jianping Shi, Chen Change Loy, Dahua Lin, and Jiaya Jia. Psanet: Point-wise spatial attention network for scene parsing. In *Proceedings of the European Conference on Computer Vision (ECCV)*, pages 267–283, 2018.
- [50] Hengshuang Zhao. semseg. <https://github.com/hszhao/semseg>, 2019.
- [51] Carl Edward Rasmussen. Gaussian processes in machine learning. In *Summer School on Machine Learning*, pages 63–71. Springer, 2003.
- [52] James S Bergstra, Rémi Bardenet, Yoshua Bengio, and Balázs Kégl. Algorithms for hyperparameter optimization. In *Advances in neural information processing systems*, pages 2546–2554, 2011.
- [53] Eric Brochu, Vlad M. Cora, and Nando de Freitas. A tutorial on bayesian optimization of expensive cost functions, with application to active user modeling and hierarchical reinforcement learning. *CoRR*, abs/1012.2599, 2010.
- [54] David Ginsbourger, Janis Janusevskis, and Rodolphe Le Riche. Dealing with asynchronicity in parallel Gaussian Process based global optimization. Research report, Mines Saint-Etienne, 2011.
- [55] Tong He, Zhi Zhang, Hang Zhang, Zhongyue Zhang, Junyuan Xie, and Mu Li. Bag of tricks for image classification with convolutional neural networks. In *The IEEE Conference on Computer Vision and Pattern Recognition (CVPR)*, June 2019.
- [56] Ekin D Cubuk, Barret Zoph, Dandelion Mane, Vijay Vasudevan, and Quoc V Le. Autoaugment: Learning augmentation strategies from data. In *Proceedings of the IEEE conference on computer vision and pattern recognition*, pages 113–123, 2019.
- [57] Mark Sandler, Andrew Howard, Menglong Zhu, Andrey Zhmoginov, and Liang-Chieh Chen. Mobilenetv2: Inverted residuals and linear bottlenecks. In *The IEEE Conference on Computer Vision and Pattern Recognition*, pages 4510–4520, 2018.
- [58] Kaiming He, Xiangyu Zhang, Shaoqing Ren, and Jian Sun. Deep residual learning for image recognition. In *The IEEE conference on computer vision and pattern recognition*, pages 770–778, 2016.

- [59] Mingxing Tan and Quoc V. Le. Efficientnet: Rethinking model scaling for convolutional neural networks. In *International Conference on Learning Representations*, pages 6105–6114, 2019.
- [60] Tsung-Yi Lin, Michael Maire, Serge Belongie, James Hays, Pietro Perona, Deva Ramanan, Piotr Dollár, and C Lawrence Zitnick. Microsoft coco: Common objects in context. In *European conference on computer vision*, pages 740–755. Springer, 2014.
- [61] Shaoqing Ren, Kaiming He, Ross Girshick, and Jian Sun. Faster r-cnn: Towards real-time object detection with region proposal networks. In *Advances in neural information processing systems*, pages 91–99, 2015.
- [62] Chao Peng, Tete Xiao, Zeming Li, Yuning Jiang, Xiangyu Zhang, Kai Jia, Gang Yu, and Jian Sun. Megdet: A large mini-batch object detector. In *Proceedings of the IEEE Conference on Computer Vision and Pattern Recognition*, pages 6181–6189, 2018.
- [63] Priya Goyal, Piotr Dollár, Ross Girshick, Pieter Noordhuis, Lukasz Wesolowski, Aapo Kyrola, Andrew Tulloch, Yangqing Jia, and Kaiming He. Accurate, large minibatch sgd: Training imagenet in 1 hour. *arXiv preprint arXiv:1706.02677*, 2017.